Electronic Supplementary Information for:

Tin(IV) Chalcogenoether Complexes as Single Source Precursors for the Chemical Vapour Deposition of SnE_2 and SnE (E = S, Se) Thin Films

Chitra Gurnani[a], Samantha L. Hawken[b], Andrew L. Hector[b], Ruomeng Huang[c], Marek Jura[d], William Levason[b], James Perkins[b], Gillian Reid[b] and Gavin B. G. Stenning[d]

a. School of Natural Sciences, Mahindra Ecole Centrale, Hyderabad, India.

b. Chemistry, University of Southampton, Southampton SO17 1BJ, UK; email: G.Reid@soton.ac.uk

c. Electronic and Computer Science, University of Southampton, Southampton SO17 1BJ, UK.

d. ISIS Neutron and Muon Source, Rutherford Appleton Laboratory, Harwell Science and Innovation Campus, Didcot, OX11 0QX, UK

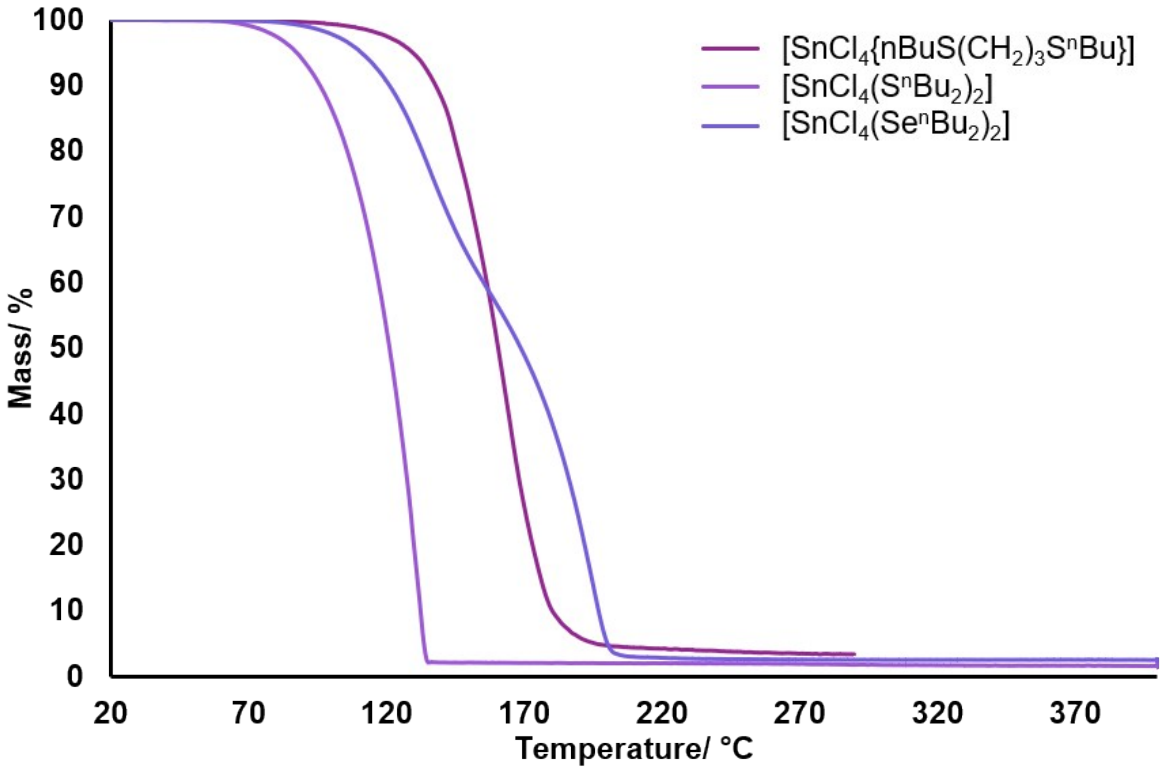

Figure S1: TGA profiles from precursors (**2**), (**3**) and (**4**)

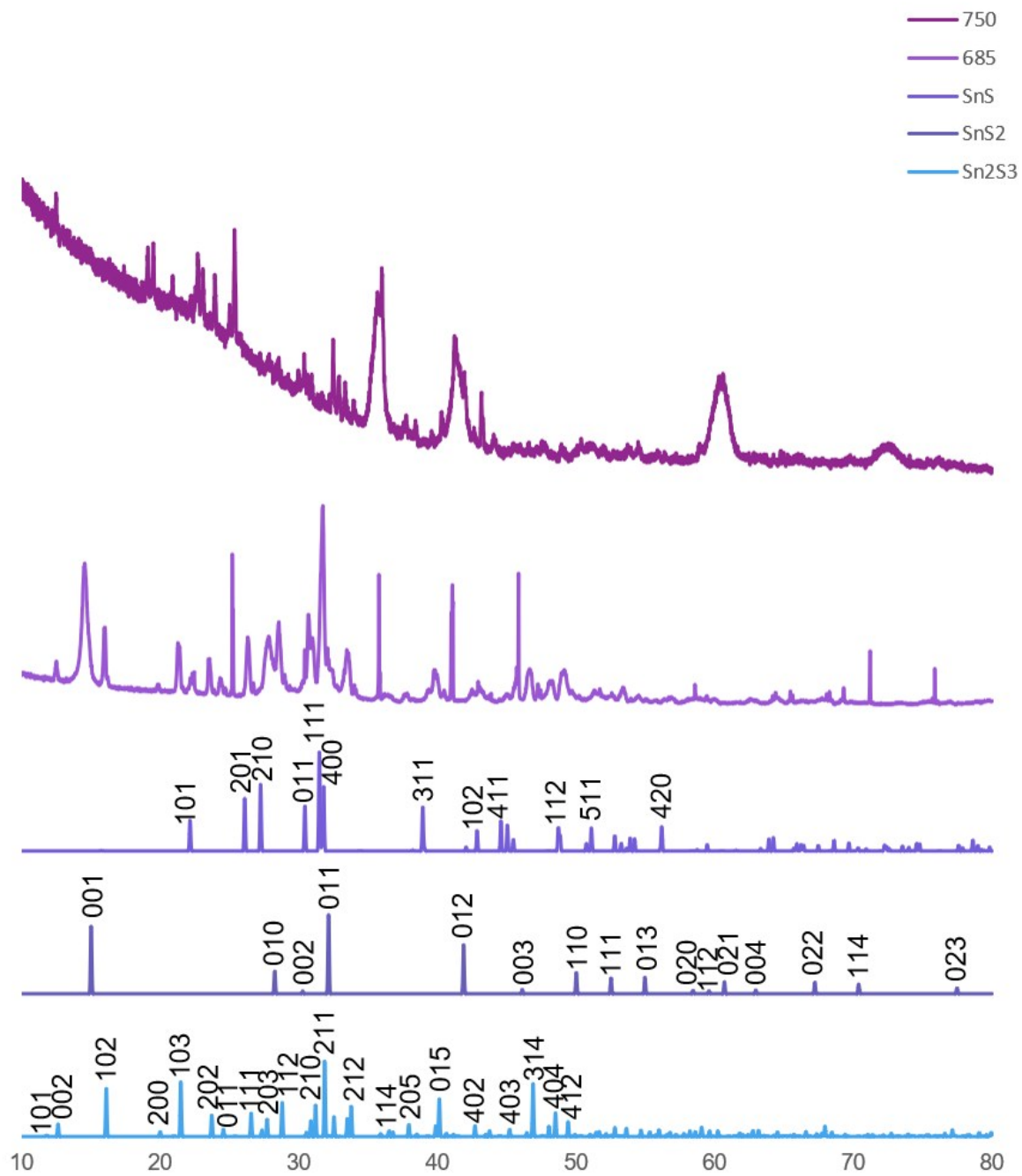
750
685
SnS
SnS2
Sn2S3
101
201
210
011
111
400
311
102
411
112
511
420
001
010
002
011
012
003
110
111
013
020
112
021
004
022
114
023
101
002
102
200
103
202
011
111
203
112
210
211
212
114
205
015
402
403
314
404
412
10
20
30
40
50
60
70
80
2θ/ degrees

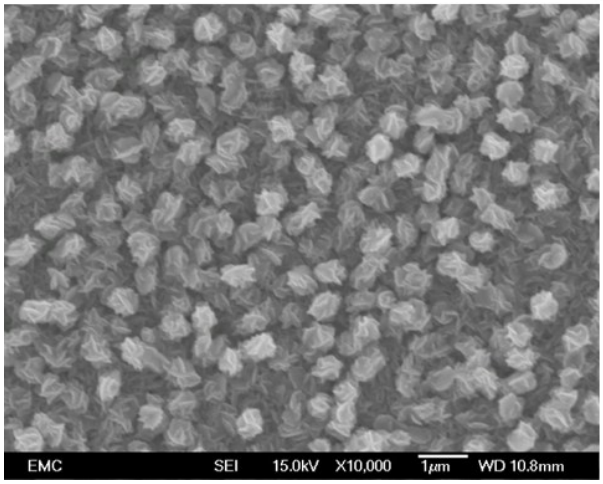
EMC SEI 15.0kV X10,000 1μm WD 10.8mm

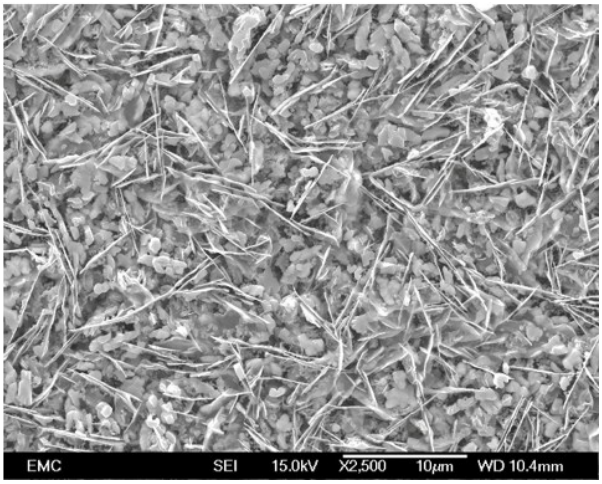
EMC SEI 15.0kV X2,500 10μm WD 10.4mm

Figure S2: (a) XRD patterns of films deposited from (**3**) at 470 °C and 395 °C with stick diagrams of diffraction patterns from bulk phases; (b) SEM image of Sn_2S_3 film and (c) SEM image of a film consisting of a mixture of Sn_2S_3 and SnS_2, deposited from (**3**) at 470 °C and 395 °C, respectively.

Element	Weight%	Atomic%
S K	34.00	65.60
Sn L	66.00	34.40
Totals	100.00	

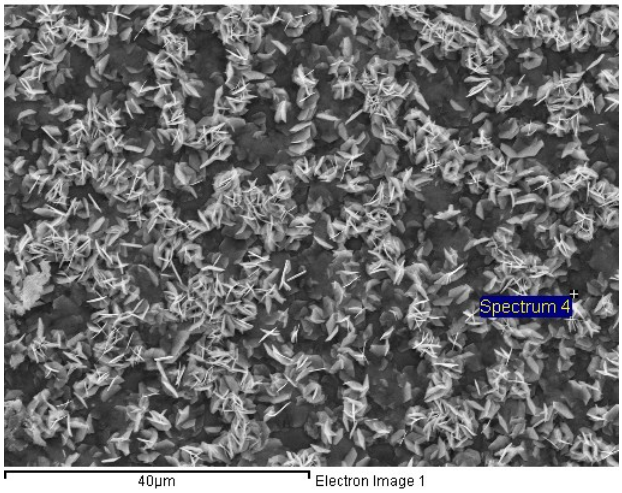

Figure S3 EDX analysis of SnS_2 film deposited from (**2**) at 286 °C

Element	Weight%	Atomic%
S K	20.83	49.35
Sn L	79.17	50.65
Totals	100.00	

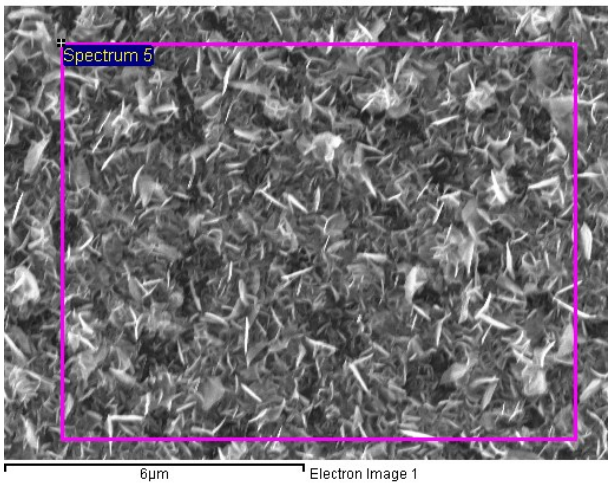

Figure S4: EDX analysis of SnS film deposited from (**2**) at 558 °C

Element	Weight%	Atomic%
Se L	56.80	66.40
Sn L	43.20	33.60
Totals	100.00	

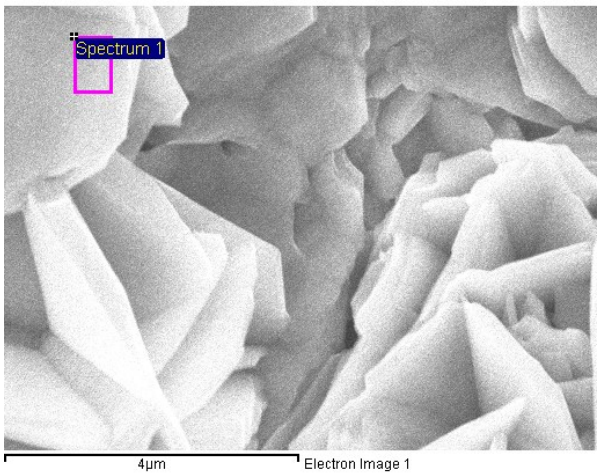

Figure S5: EDX analysis of $SnSe_2$ film deposited from (**4**) at 325 °C

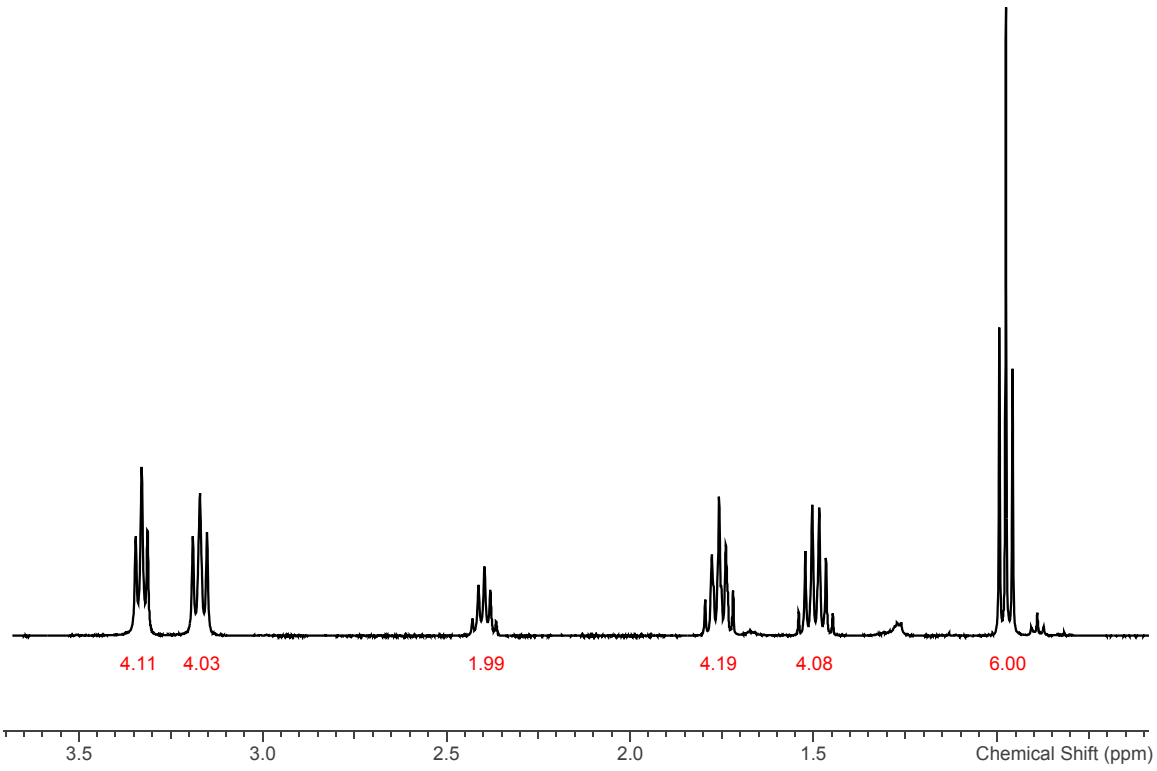

Figure S6: Room temperature ^{1}H NMR spectrum of $[SnCl_4\{^nBuS(CH_2)_3S^nBu\}]$ ($CDCl_3$, 25 °C).

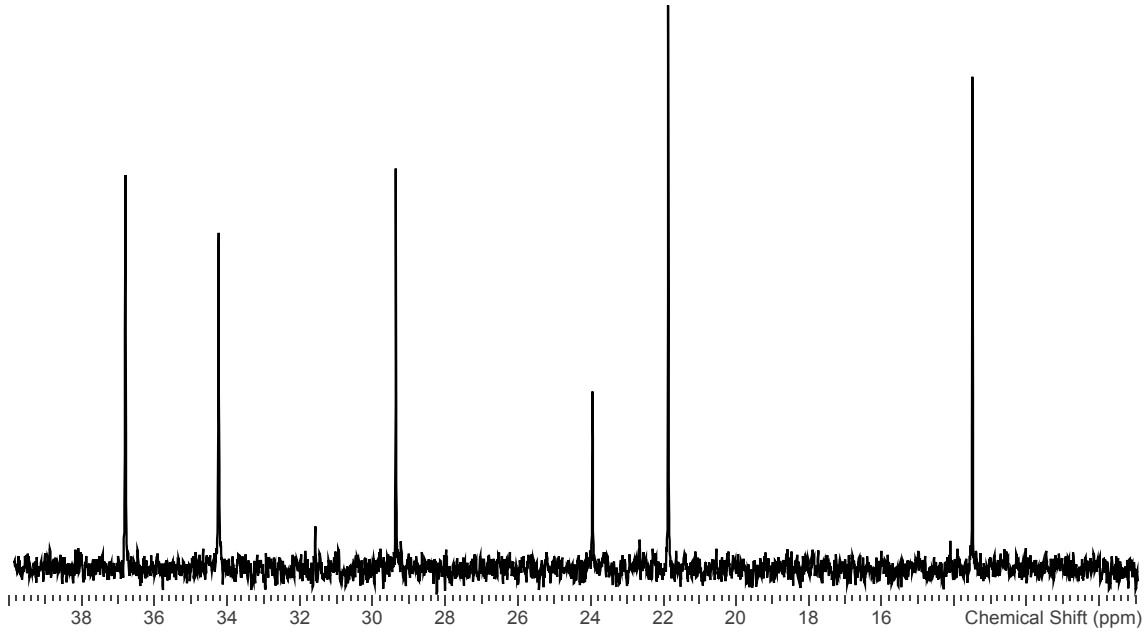

Figure S7: Room temperature $^{13}C\{^{1}H\}$ NMR spectrum of $[SnCl_4\{^{n}BuS(CH_2)_3S^{n}Bu\}]$ ($CDCl_3$, 25 °C).

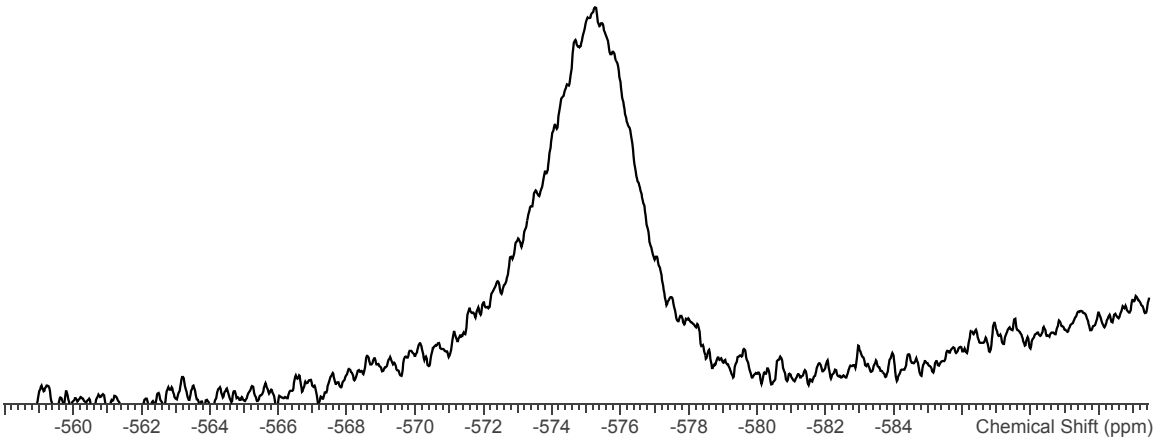

Figure S8: Room temperature ^{119}Sn NMR spectrum of $[SnCl_4\{^{n}BuS(CH_2)_3S^{n}Bu\}]$ (CH_2Cl_2, 25 °C).

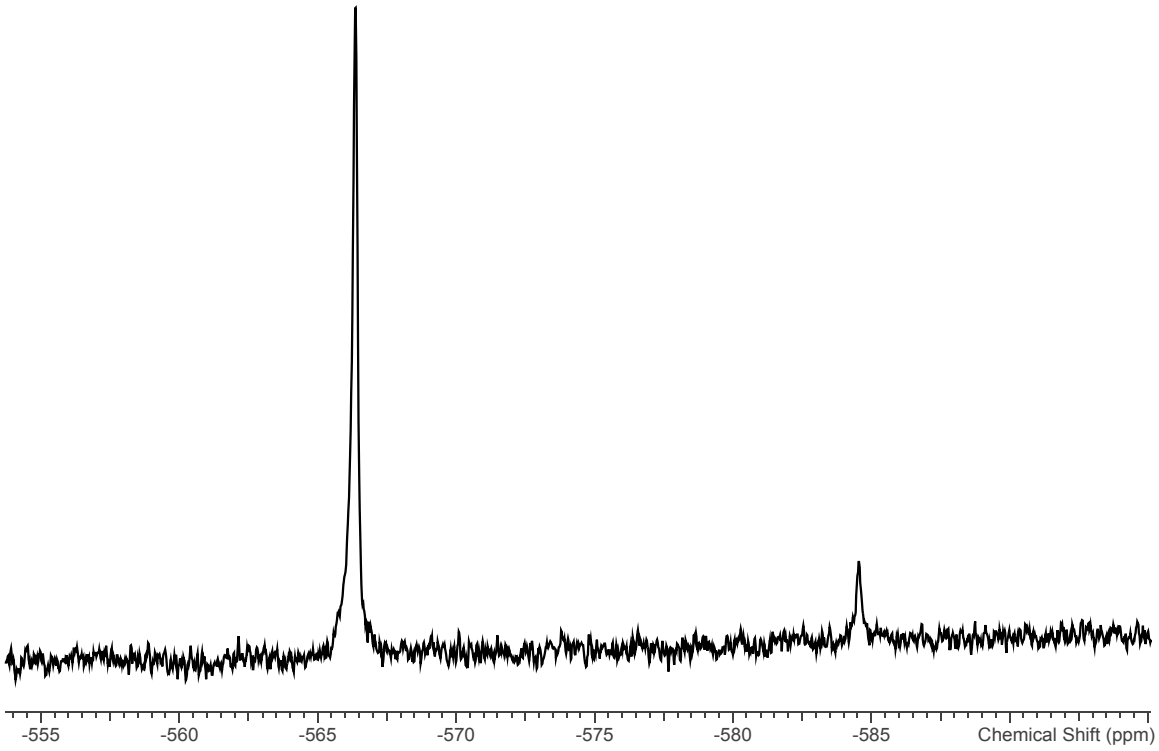

Figure S9: Low temperature ^{119}Sn NMR spectrum of [$SnCl_4${^{n}BuS$(CH_2)_3$S^{n}Bu}] (CH_2Cl_2, –90 °C).

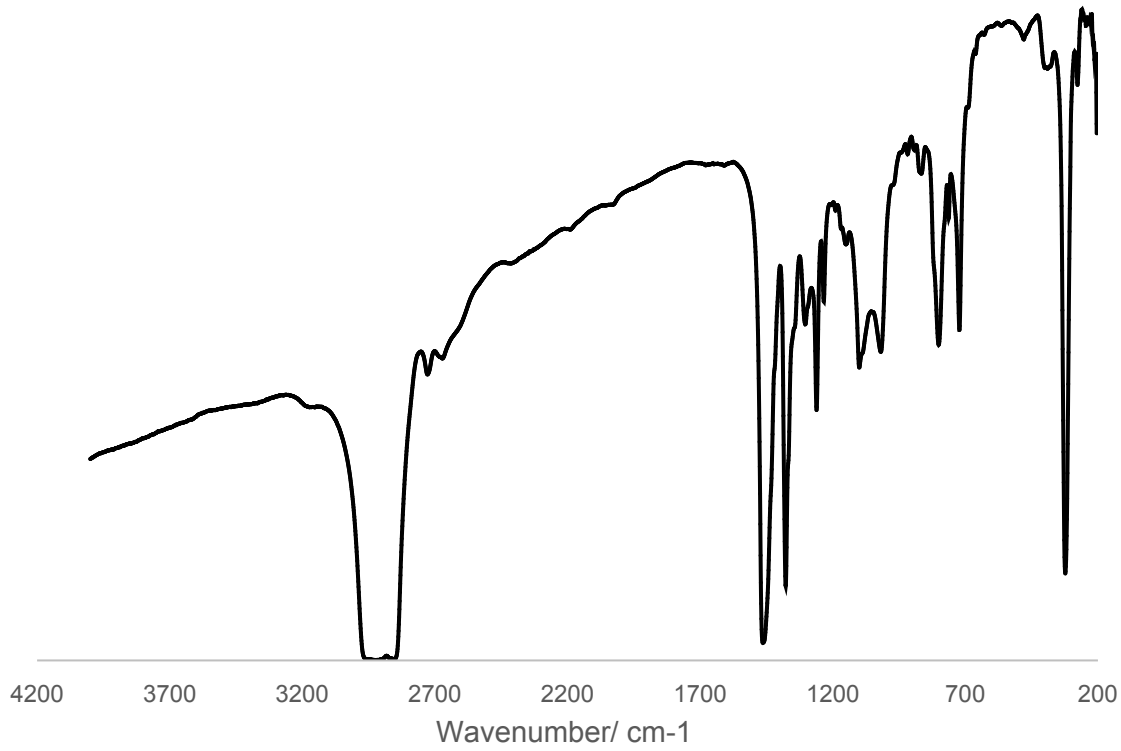

Figure S10: IR spectrum of [$SnCl_4${^{n}BuS$(CH_2)_3$S^{n}Bu}] as a Nujol mull between CsI plates

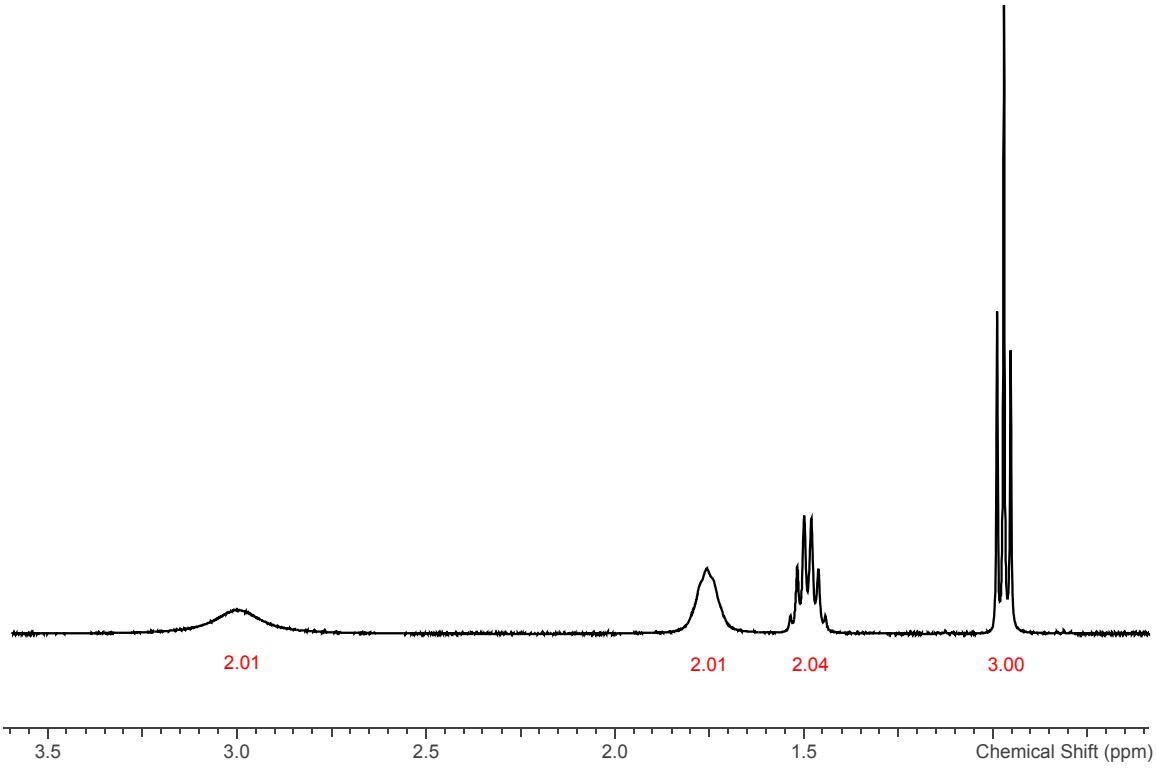

Figure S11: Room temperature ^{1}H NMR spectrum of $[SnCl_4(S^nBu_2)_2]$ ($CDCl_3$, 25 °C).

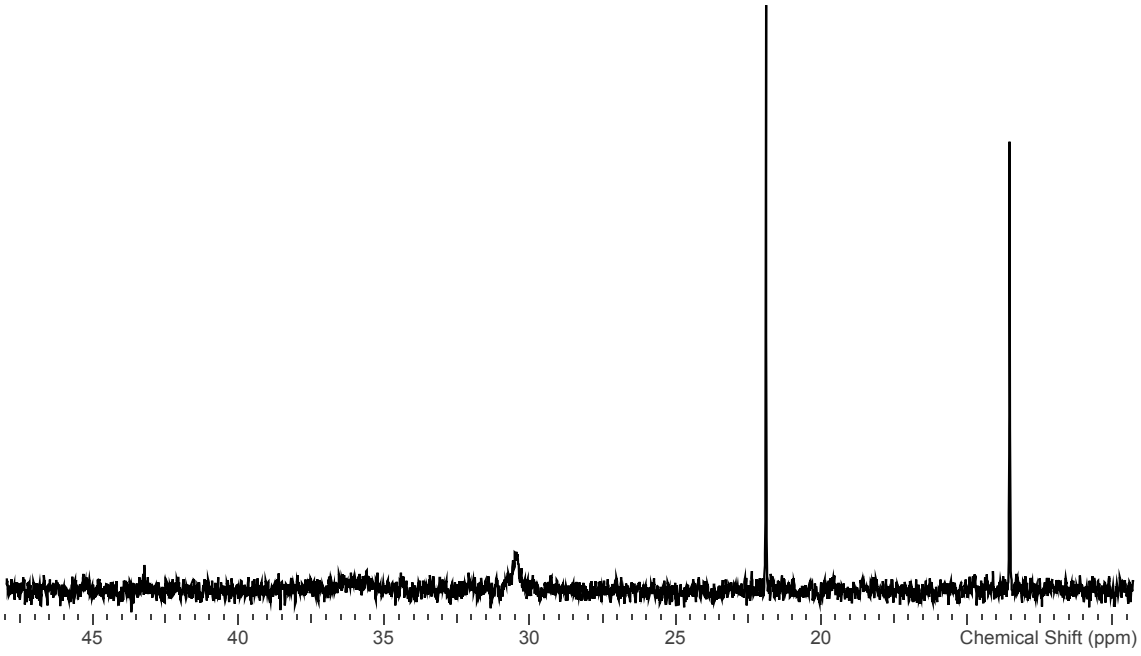

Figure S12: Showing the room temperature $^{13}C\{^{1}H\}$ NMR spectrum of $[SnCl_4(S^nBu_2)_2]$ ($CDCl_3$, 25 °C).

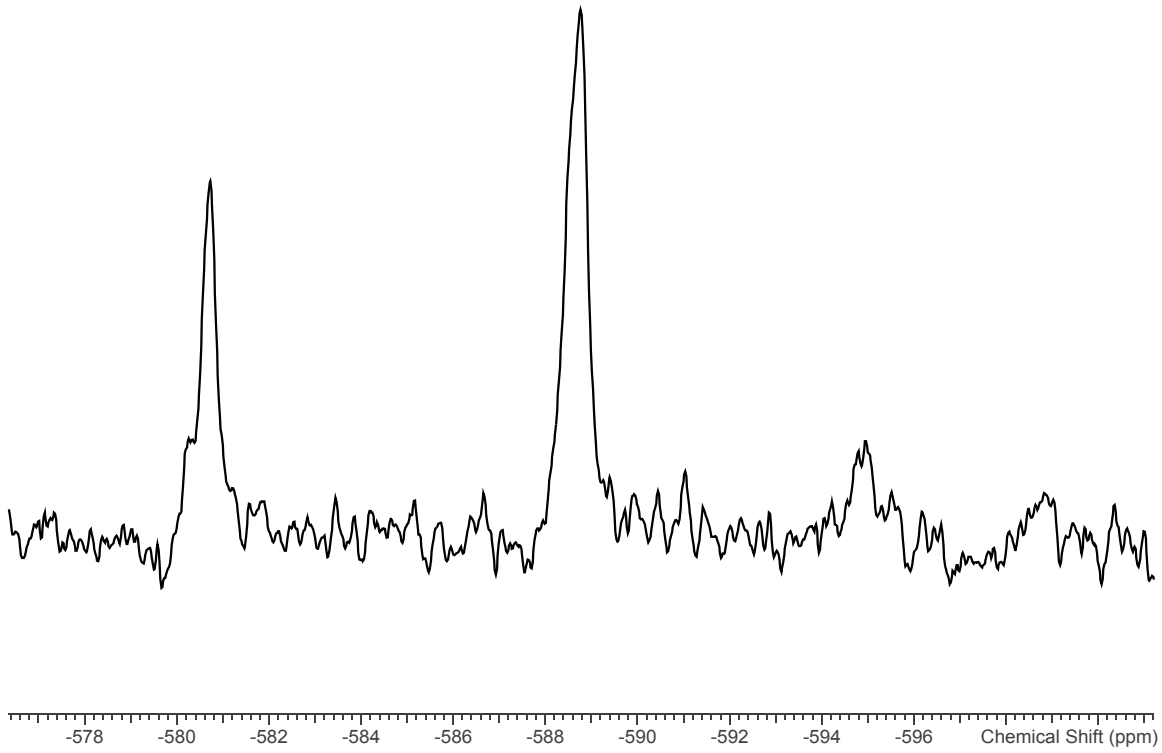

Figure S13: Showing the low temperature ^{119}Sn NMR spectrum of $[SnCl_4(S^nBu_2)_2]$ (CH_2Cl_2, –50 °C).

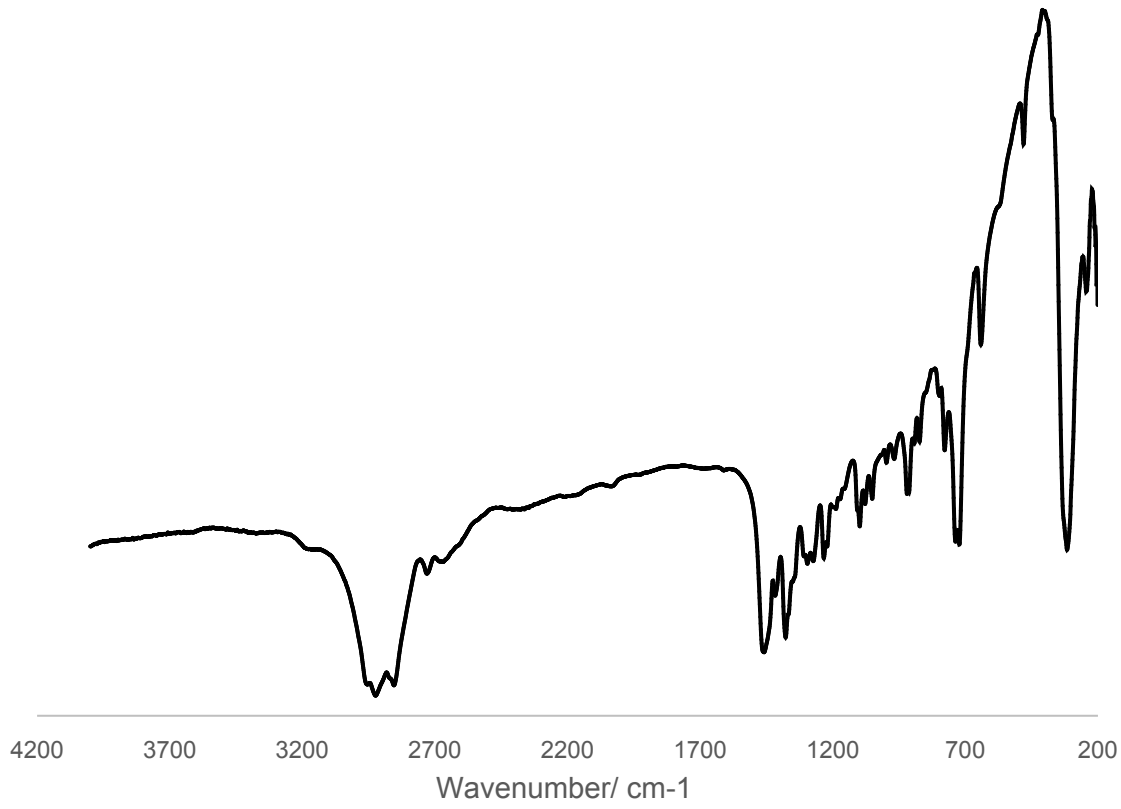

Figure S14: Showing the IR spectrum of $[SnCl_4(S^nBu_2)_2]$ as a Nujol mull between CsI plates.

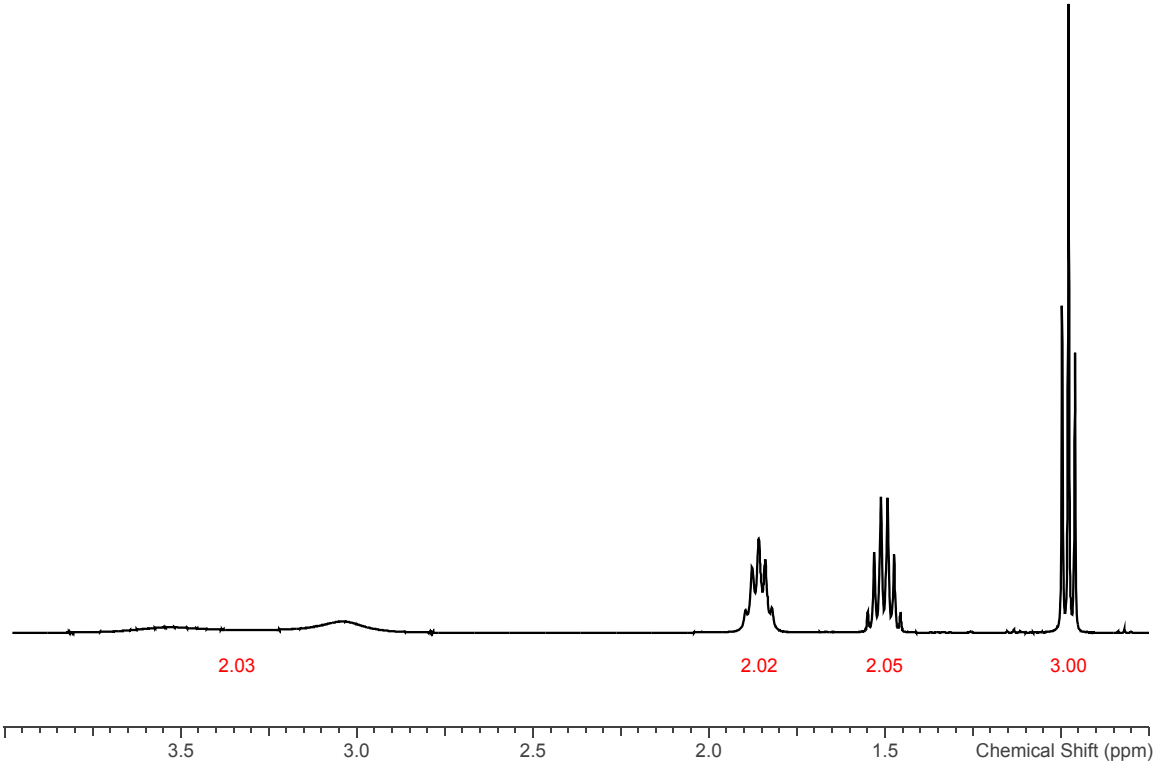

Figure S15: Room temperature ^{1}H NMR spectrum of $[SnCl_4(Se^nBu_2)_2]$. ($CDCl_3$, 25 °C).

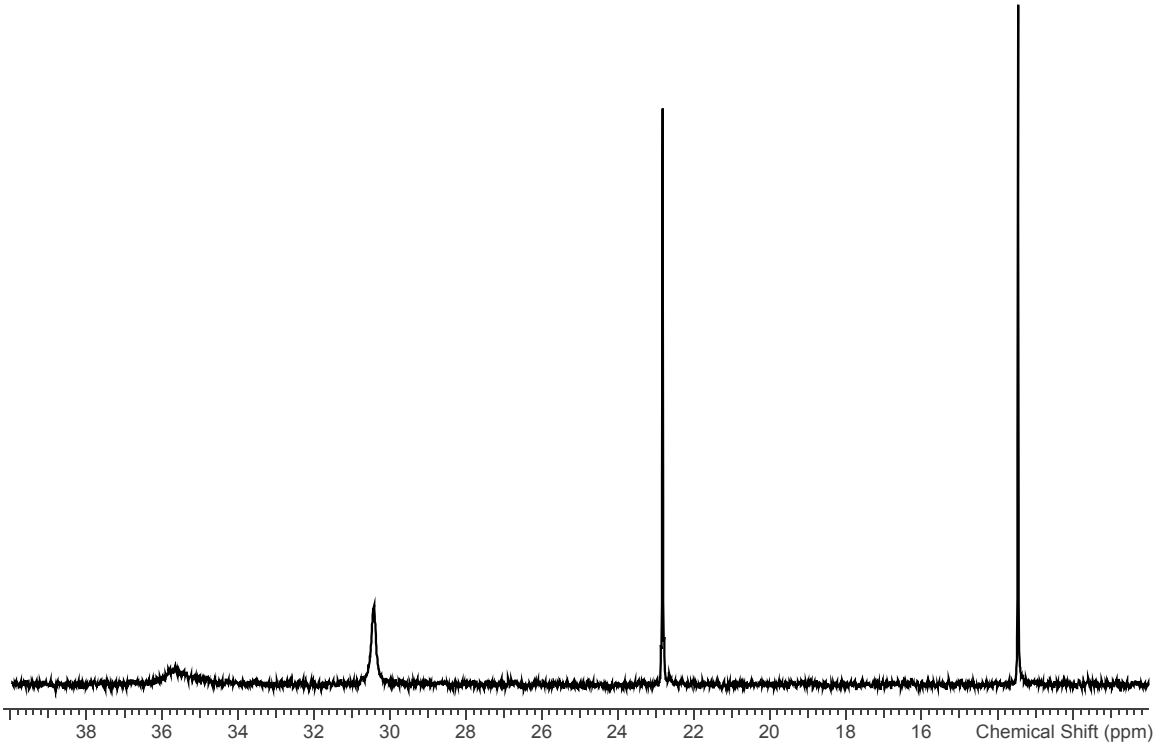

Figure S16: Room temperature $^{13}C\{^{1}H\}$ NMR spectrum of $[SnCl_4(Se^nBu_2)_2]$ ($CDCl_3$, 25 °C).

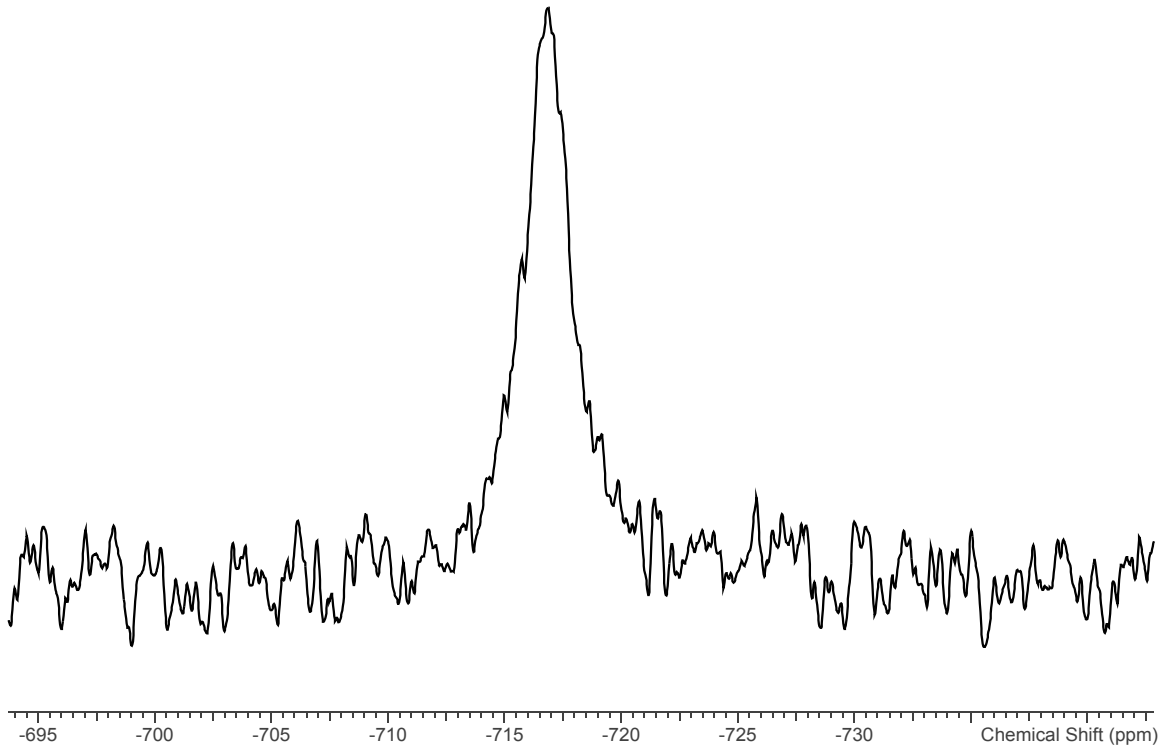

Figure S17: Room temperature ^{119}Sn NMR spectrum of $[SnCl_4(Se^nBu_2)_2]$ (CH_2Cl_2, 25 °C).

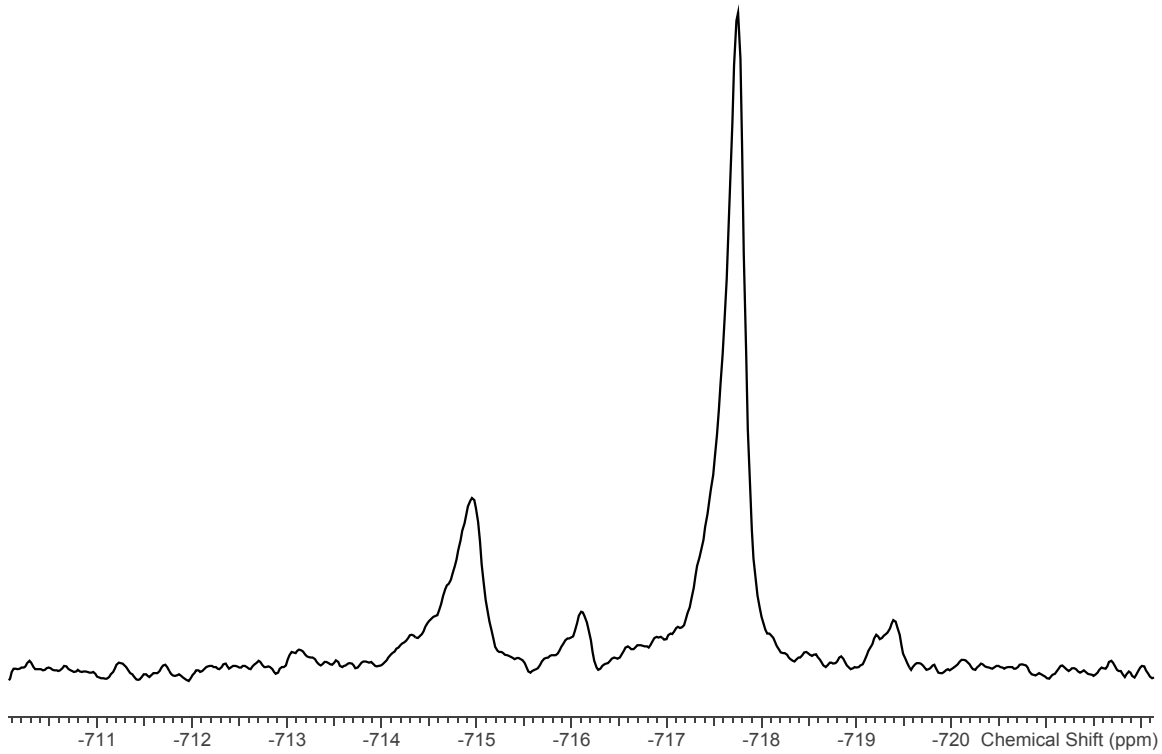

Figure S18: Low temperature ^{119}Sn NMR spectrum of $[SnCl_4(Se^nBu_2)_2]$ (CH_2Cl_2, −90 °C).

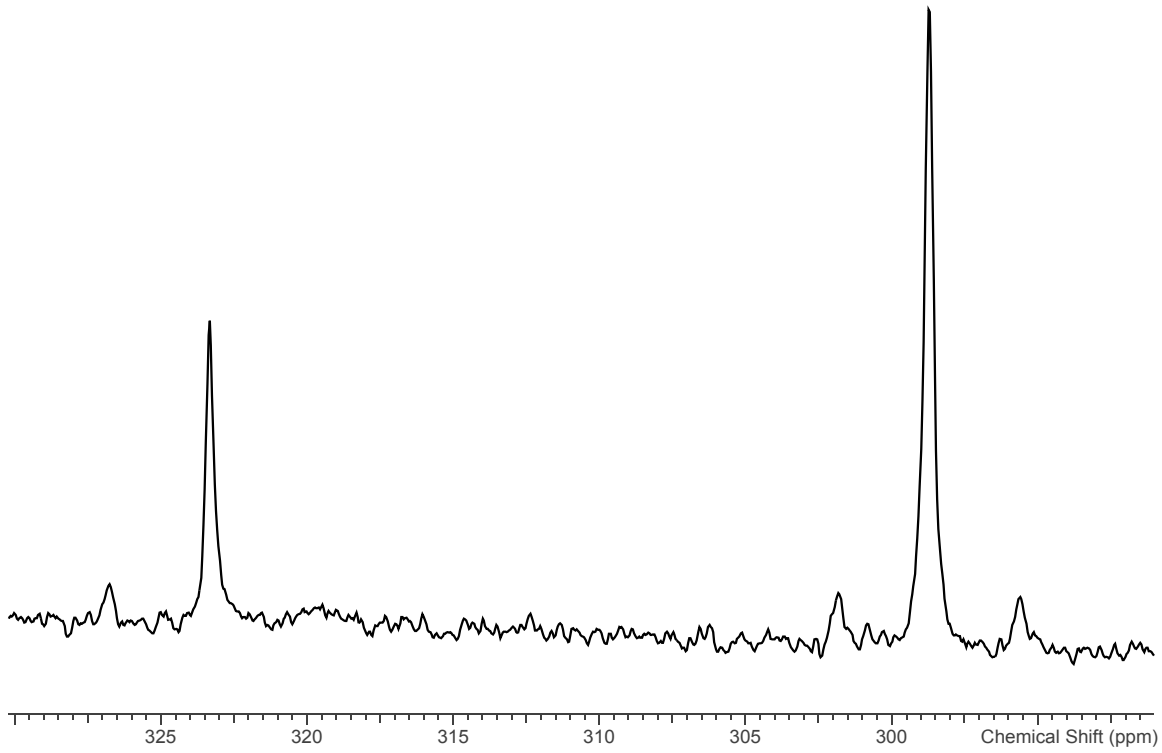

Figure S19: Low temperature $^{77}Se\{^{1}H\}$ NMR spectrum of $[SnCl_4(Se^nBu_2)_2]$ (CH_2Cl_2, −90 °C).

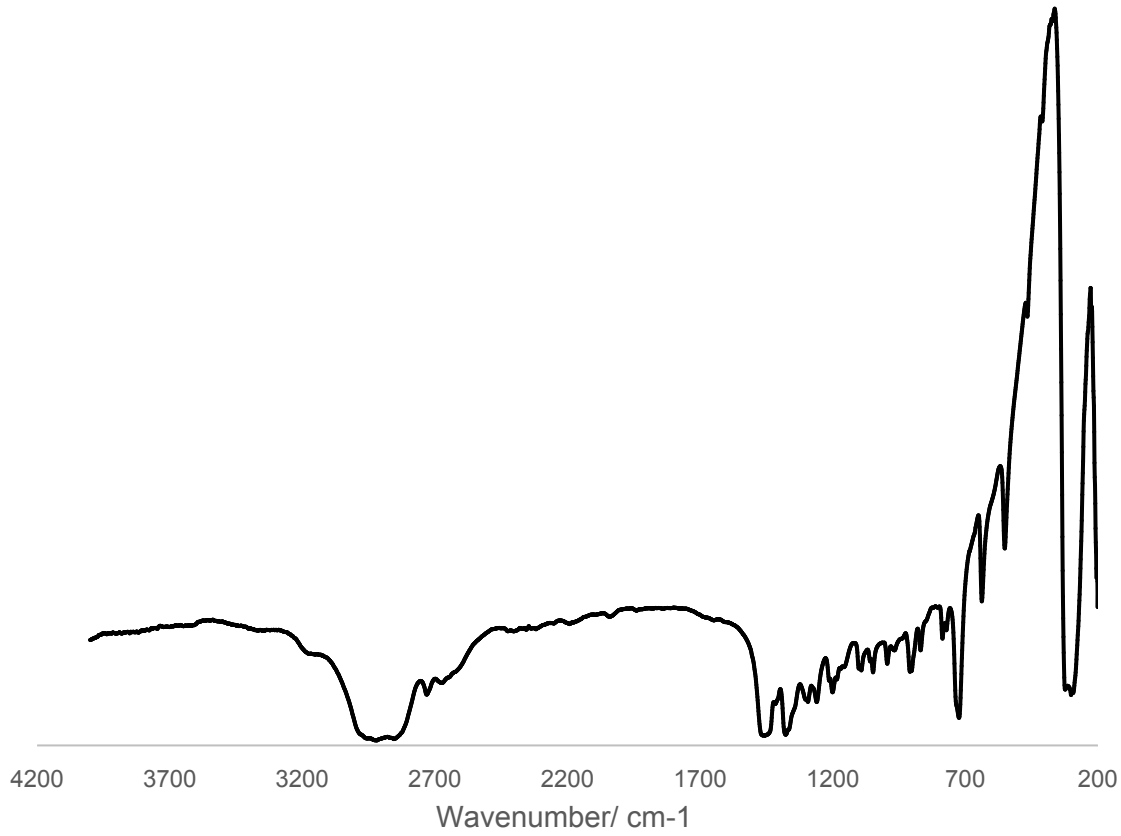

Figure S20: IR spectrum of $[SnCl_4(Se^nBu_2)_2]$ as a Nujol mull between CsI plates.